

# Antiferromagnetic order in systems with doublet $S_{\text{tot}} = 1/2$ ground states

Sambuddha Sanyal,<sup>1</sup> Argha Banerjee,<sup>1</sup> Kedar Damle,<sup>1</sup> and Anders W. Sandvik<sup>2</sup>

<sup>1</sup>*Department of Theoretical Physics, Tata Institute of Fundamental Research, Mumbai 400005, India.*

<sup>2</sup>*Department of Physics, Boston University, 590 Commonwealth Avenue, Boston, Massachusetts 02215, USA.*

We use projector Quantum Monte-Carlo methods to study the  $S_{\text{tot}} = 1/2$  doublet ground states of two dimensional  $S = 1/2$  antiferromagnets on a  $L \times L$  square lattice with an odd number of sites  $N_{\text{tot}} = L^2$ . We compute the ground state spin texture  $\Phi^z(\vec{r}) = \langle S^z(\vec{r}) \rangle_{\uparrow}$  in  $|G\rangle_{\uparrow}$ , the  $S_{\text{tot}} = 1/2$  component of this doublet, and investigate the relationship between  $n^z$ , the thermodynamic limit of the staggered component of this ground state spin texture, and  $m$ , the thermodynamic limit of the magnitude of the staggered magnetization vector of the same system in the singlet ground state that obtains for even  $N_{\text{tot}}$ .  $n^z$  and  $m$  would have been equal if the non-zero value of  $S_{\text{tot}}^z$  in  $|G\rangle_{\uparrow}$  caused the direction of the staggered magnetization vector to be fully pinned in the thermodynamic limit. By studying several different deformations of the square lattice Heisenberg antiferromagnet, we establish that this is not the case. For the sizeable range of  $m$  accessed in our numerics, we find a universal relationship between the two, that is independent of the microscopic details of the lattice level Hamiltonian and can be well approximated by a polynomial interpolation formula:  $n^z \approx (\frac{1}{3} - \frac{a}{2} - \frac{b}{4})m + am^2 + bm^3$ , with  $a \approx 0.288$  and  $b \approx -0.306$ . We also find that the full spin texture  $\Phi^z(\vec{r})$  is itself dominated by Fourier modes near the antiferromagnetic wavevector in a universal way. On the analytical side, we explore this question using spin-wave theory, a simple mean field model written in terms of the total spin of each sublattice, and a rotor model for the dynamics of  $\vec{n}$ . We find that spin-wave theory reproduces this universality of  $\Phi^z(\vec{r})$  and gives  $n^z = (1 - \alpha - \beta/S)m + (\alpha/S)m^2 + \mathcal{O}(S^{-2})$  with  $\alpha \approx 0.013$  and  $\beta \approx 1.003$  for spin- $S$  antiferromagnets, while the sublattice-spin mean field theory and the rotor model both give  $n^z = \frac{1}{3}m$  for  $S = 1/2$  antiferromagnets. We argue that this latter relationship becomes asymptotically exact in the limit of infinitely long-range *unfrustrated* exchange interactions.

PACS numbers: 75.10.Jm 05.30.Jp 71.27.+a

## I. INTRODUCTION

Computational studies of strongly correlated systems necessarily involve an extrapolation to the thermodynamic limit from a sequence of finite sizes at which calculations are feasible. Understanding,<sup>1</sup> and at times reducing,<sup>2</sup> these finite-size corrections to the thermodynamic limit is thus an important aspect of any such calculation. For instance, the best estimates of  $m$ , the magnitude of the ground state Néel order parameter in the thermodynamic limit of the two-dimensional  $S = 1/2$  square lattice Heisenberg antiferromagnet rely on a sequence of  $L_x \times L_y$  systems with even length  $L_x$  ( $L_y$ ) in the  $x$  ( $y$ ) direction and periodic boundary conditions in both directions.<sup>3,4</sup> Other studies suggest<sup>2</sup> that it is some times advantageous to use “cylindrical” samples with periodic boundary conditions in one direction and pinned boundary conditions in the other direction, whereby spins are held fixed by the use of pinning fields on one pair of edges—this choice also allows for a very accurate determination of ground-state parameters such as  $m$  for specific values<sup>2</sup> of the aspect ratio  $L_y/L_x$ .

All these approaches focus on systems with an *even* number of spin-half variables; this choice allows the ground-state of the finite system to lie in the singlet sector favoured by unfrustrated antiferromagnetic interactions.<sup>5</sup> Although not commonly used, another choice is certainly possible: Namely, one could in principle consider antiferromagnets on a  $L \times L$  square lattice with an odd number  $N_{\text{tot}} = L^2$  of spin-half moments.

Such a system is expected to have a doublet ground state with total spin  $S_{\text{tot}} = 1/2$ . Focusing on the  $S_{\text{tot}}^z = 1/2$  member  $|G\rangle_{\uparrow}$  of this doublet, one could examine the ground state spin texture defined by  $\Phi^z(\vec{r}) \equiv \langle S_{\vec{r}}^z \rangle_{\uparrow}$  (where  $\langle \dots \rangle_{\uparrow}$  refers to expectation values in  $|G\rangle_{\uparrow}$ ), and use the antiferromagnetic component of this spin texture, defined as

$$n^z = \frac{1}{N_{\text{tot}}} \sum_{\vec{r}} \eta_{\vec{r}} \langle S_{\vec{r}}^z \rangle_{\uparrow}, \quad (1)$$

to obtain information about the antiferromagnetic ordering in the system (here  $\eta_{\vec{r}} = +1$  on the  $A$  sublattice and  $-1$  on the  $B$  sublattice).

Clearly,  $n^z$  provides a measure of antiferromagnetic order that is quite distinct from the conventional order parameter  $m$ , which can be defined, e.g., according to

$$m^2 = \frac{1}{N_{\text{tot}}} \sum_{\vec{r}, \vec{r}'} \eta_{\vec{r}} \eta_{\vec{r}'} \langle \vec{S}_{\vec{r}} \cdot \vec{S}_{\vec{r}'} \rangle_0, \quad (2)$$

where  $\langle \dots \rangle_0$  denotes averages in the singlet ground state realized for even  $N_{\text{tot}}$ . The relationship between the thermodynamic-limit values of  $n^z$  and  $m$  is a fundamental aspect of the spontaneously broken  $SU(2)$  symmetry of the Néel state. However, not much is known about it beyond the fact that  $n^z$  is *significantly smaller than*  $m$  for the nearest neighbour Heisenberg antiferromagnet on the square lattice.<sup>6</sup> Here, we provide a more detailed characterization of this relationship.

Our basic result is that  $n^z$  is determined in a universal way by the value of  $m$ . In other words,  $n^z$  plotted against  $m$  for several different deformations of the  $S = 1/2$  square lattice Heisenberg antiferromagnet falls on a single curve which defines a universal function that is insensitive to the microscopic details of the model Hamiltonian. This universal function is well-approximated by a polynomial interpolation formula:

$$n^z \approx \left(\frac{1}{3} - \frac{a}{2} - \frac{b}{4}\right)m + am^2 + bm^3, \quad (3)$$

with  $a \approx 0.288$  and  $b \approx -0.306$ . In addition, we also find that the full spin texture  $\Phi^z(\vec{r})$  is dominated by Fourier modes near the antiferromagnetic wave-vector in a universal way independent of microscopic details. We show that this universality is captured by spin-wave theory, which also predicts

$$n^z = (1 - \alpha - \beta/S)m + (\alpha/S)m^2 + \mathcal{O}(S^{-2}), \quad (4)$$

with  $\alpha \approx 0.013$  and  $\beta \approx 1.003$  for spin- $S$  antiferromagnets. In addition, we explore two other ways of thinking about this universal function. One of them is a mean field theory formulated in terms of the total spin of each sublattice, while the other approach is in terms of a quantum rotor Hamiltonian for the Néel vector  $\vec{n}$  of a system with an odd number of sites. Both these give

$$n^z = \frac{m}{3} \quad (5)$$

for  $S = 1/2$  antiferromagnets, which is close to the observed relationship but not exactly right. We argue that this latter estimate (Eqn. 5) will become asymptotically exact in the limit of infinitely long-range *unfrustrated* exchange interactions. In this limit, we also expect  $m \rightarrow 1/2$ , and our polynomial fit to the universal function  $n^z(m)$  was therefore constrained to ensure that  $n^z \rightarrow m/3$  when  $m \rightarrow 1/2$ .

The outline of the rest of the paper is as follows: In Section II we define various deformations of the square lattice  $S = 1/2$  Heisenberg antiferromagnet. In Section III, we outline the projector quantum Monte Carlo (QMC) method used in this study, and then discuss in some detail our QMC results for  $n^z$  as well as the full spin texture  $\Phi^z(\vec{r})$ , focusing on the universal properties alluded to earlier. In Section IV, we outline three analytical approaches to the relationship between  $n^z$  and  $m$ . The first is a large- $S$  spinwave expansion, within which we calculate the ground state spin texture  $\Phi^z(\vec{r})$  and its antiferromagnetic Fourier component  $n^z$  to leading  $\mathcal{O}(1/S)$  order, and demonstrate that such a calculation also yields the universality properties summarized earlier, but does not provide a quantitatively accurate account of the QMC results for  $\Phi^z(\vec{r})$  or  $n^z(m)$ . The second is a mean-field theory formulated in terms of the total spin of each sublattice. And the third approach is in terms of a quantum rotor Hamiltonian which is expected to correctly describe the low-energy tower of states for odd  $N_{\text{tot}}$ . In Section V, we conclude with some speculations about a possible effective field theory approach to the calculation of  $\Phi^z(\vec{r})$ .

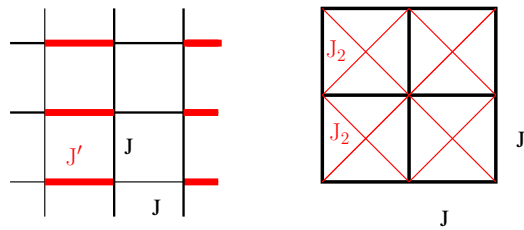


FIG. 1: An illustration of the interactions present in the  $JJ'$  (left panel) and  $JJ_2$  (right panel) model Hamiltonians. In this illustration, black bonds denote exchange interaction strength of  $J$ , while a red bond represents exchange strength of  $J'$  ( $J_2$ ) in the left (right) panel

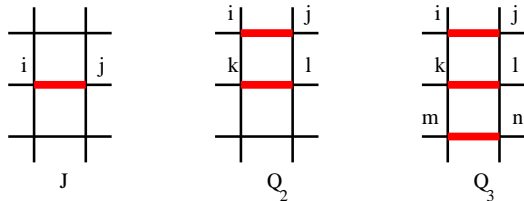


FIG. 2: Bond and plaquette operators in  $JQ$  model Hamiltonians. A thick bond denotes a bipartite projector acting on that bond. All possible orientations of these bond and plaquette operators are allowed.

## II. MODELS

We consider four deformations of the square lattice  $S = 1/2$  nearest neighbour Heisenberg antiferromagnet; all four retain the full  $SU(2)$  spin rotation symmetry of the original model.

The first of these models is the coupled-dimer antiferromagnet, in which there are two kinds of nearest neighbour interactions  $J$  and  $J'$ , as shown in Fig. 1 (left panel), where the ratio  $\alpha = J'/J$  can be tuned from  $\alpha = 1$  to  $\alpha = \alpha_c \approx 1.90$  at which collinear antiferromagnetic order is lost.<sup>7</sup> The Hamiltonian for this system reads:

$$H_{JJ'} = J \sum_{\langle ij \rangle} \mathbf{S}_i \cdot \mathbf{S}_j + J' \sum_{\langle ij \rangle'} \mathbf{S}_i \cdot \mathbf{S}_j, \quad (6)$$

where  $\langle ij \rangle$  ( $\langle ij \rangle'$ ) denotes a pair of nearest neighbour sites connected by a black (red) bond (see Fig. 1). Another deformation of the Heisenberg model, the  $JJ_2$  model, has additional next nearest neighbour Heisenberg exchange interactions  $J_2$ , as shown in Fig. 1 (right panel). The Hamiltonian reads

$$H_{JJ_2} = J \sum_{\langle ij \rangle} \mathbf{S}_i \cdot \mathbf{S}_j + J_2 \sum_{\langle\langle ij \rangle\rangle} \mathbf{S}_i \cdot \mathbf{S}_j, \quad (7)$$

where  $\langle\langle ij \rangle\rangle$  denotes a pair of next nearest neighbour sites. Both these are amenable to straightforward spin-wave theory analyses, and the coupled dimer model can also be studied numerically to obtain numerically exact results even for very large sizes due to the absence of any

sign problems in Quantum Monte Carlo studies. However, exact numerical results on the  $JJ_2$  model are restricted to small sizes since Quantum Monte Carlo methods encounter a sign problem when dealing with next-nearest neighbour interactions on the square lattice.

In addition, we study two generalizations that involve additional multispin interactions; the “ $JQ$ ” models.<sup>8,9</sup> Of these, the  $JQ_2$  model has 4-spin interactions in addition to the usual Heisenberg exchange terms, and is defined by the Hamiltonian

$$H_{JQ_2} = -J \sum_{\langle ij \rangle} P_{ij} - Q_2 \sum_{\langle ij, kl \rangle} P_{ij} P_{kl}, \quad (8)$$

where the plaquette interaction  $Q_2$  involves two adjacent parallel bonds on the square lattice as shown in Fig. 2 (middle panel) and

$$P_{ij} = \frac{1}{4} - \mathbf{S}_i \cdot \mathbf{S}_j \quad (9)$$

is a bipartite singlet projector. The first term in Eqn. 8 is just the standard Heisenberg exchange. Similarly, the  $JQ_3$  model has 6-spin interactions and is defined by the Hamiltonian

$$H_{JQ_3} = -J \sum_{\langle ij \rangle} P_{ij} - Q_3 \sum_{\langle ij, kl, nm \rangle} P_{ij} P_{kl} P_{nm}, \quad (10)$$

where the plaquette interactions now involve three adjacent parallel bonds on the square lattice, as shown in Fig. 2 (right panel). The products of singlet projectors making up the  $Q_2$  and  $Q_3$  terms tend to reduce the Néel order of the ground state, and, when sufficiently strong, lead to a quantum phase transition into a valence-bond-solid state.<sup>8,9</sup> Here we stay within the Néel state in both models, and study universal aspects of this state as the Néel order is weakened.

### III. PROJECTOR QMC STUDIES

We use the total spin-half sector version<sup>10</sup> of the valence-bond basis projector QMC method<sup>11,12</sup> to study  $L \times L$  samples with  $L$  odd and free boundary conditions. We compute  $\Phi^z(\vec{r})$  and  $n^z$  in such samples for the  $JJ'$  model and  $JQ$  models in their antiferromagnetic phase. We also study the same models on  $L \times L$  lattices with  $L$  even and periodic boundary conditions using the original singlet sector valence bond projector QMC method. In both cases we use the most recent formulation with very efficient loop updates.<sup>10,12</sup> Our system sizes range from  $L = 11$  to  $L = 101$ , and projection power scales as  $L^3$  to ensure convergence to the ground state. We perform  $\gtrsim 10^5$  equilibration steps followed by  $\gtrsim 10^6$  Monte Carlo measurements to ensure that statistical and systematic errors are small.

Data for  $n^z$  from a sequence of  $L \times L$  systems with  $L$  odd shows that  $n^z$  extrapolates to a finite value in the

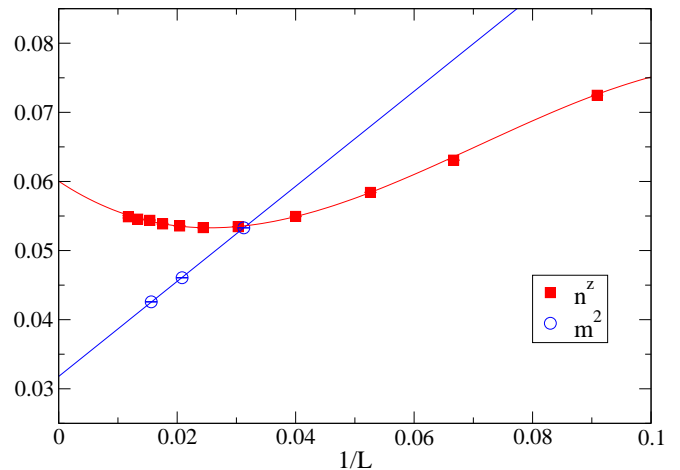


FIG. 3: An illustrative example of finite size corrections of  $n^z$  and  $m^2$ , observed in the antiferromagnetic phase of the  $JJ'$  model ( $J' = 1.8$ ). Note the non-monotonic behaviour of finite size corrections for  $n^z$ , which is fitted to a cubic polynomial. In contrast, finite size data for  $m^2$  is well described by a linear dependence on  $1/L$ .

$L \rightarrow \infty$  limit as long as the system is in the antiferromagnetic phase. However, we find that the approach of this observable to the thermodynamic limit has a non-monotonic behaviour. To obtain accurate extrapolations to infinite size, it is therefore necessary to fit the finite size data to a third-order polynomial in  $1/L$ . We find that the coefficient for the leading  $1/L$  term in this polynomial is rather small; this is true for all the models studied here, as long as they remain in the antiferromagnetic phase. In Fig. 3 and Fig. 4, we show examples of this behaviour of the finite size corrections in  $n^z$ . In these figures, we also show the approach to the thermodynamic limit for  $m$ , as measured in a sequence of periodic  $L \times L$  systems with  $L$  even. We find that in complete contrast to the behaviour of  $n^z$ ,  $m$  extrapolates monotonically to the thermodynamic limit, with a dominant  $1/L$  dependence—this is consistent with previous studies of the structure factor in square lattice antiferromagnets<sup>12</sup> (however, with spatially anisotropic couplings, one can also observe strong non-monotonicity in  $m$ <sup>13</sup>).

The non-zero value of  $n^z$  in the thermodynamic limit clearly reflects the long-range antiferromagnetic order present in the system and a partial breaking of the  $SU(2)$  symmetry (due to the fact that we study only one member of the doublet ground state). For periodic systems, the same long range antiferromagnetic order is captured by the non-zero value of  $m$  in the large  $L$  limit—and a calculation of  $m$  (through  $\langle m^2 \rangle$ ) for the odd- $L$  systems with periodic boundaries would of course lead to the same value. However, since  $m \neq n^z$ , the full staggered magnetization is not forced to lie along the  $z$  spin axis, and it is interesting to ask: What is the relationship between these two measures of antiferromagnetic order? Our numerical data are unequivocal as far as this relationship is

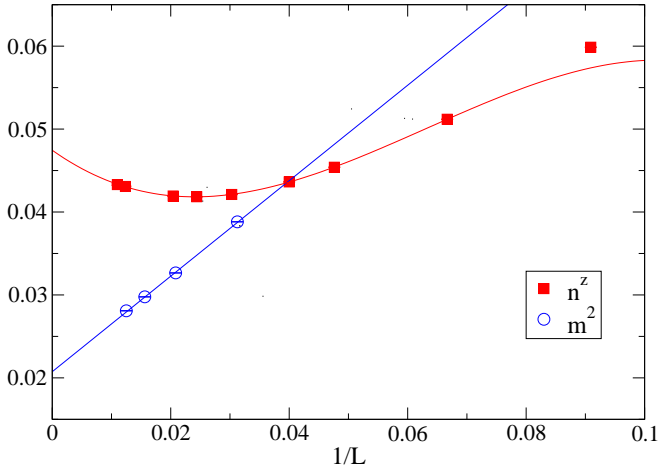


FIG. 4: Another illustrative example of finite size corrections of  $n^z$  and  $m^2$ , observed in the antiferromagnetic phase of  $JQ_2$  model at  $Q_2 = 1.0$ . Again, note the non-monotonic behaviour of finite size corrections for  $n^z$ , which is fitted to a cubic polynomial (only  $L > 20$  data used in the fit). In contrast, finite size data for  $m^2$  is well described by a linear dependence on  $1/L$ .

concerned, as is clear from Fig. 5, which shows a plot of  $n^z$  versus  $m$  in the thermodynamic limit of the  $JJ'$ ,  $JQ_2$  and  $JQ_3$  models. Here *each* point represents the result of a careful extrapolation similar to the examples shown in Fig. 3 and Fig. 4, and provides an accurate estimate of the corresponding thermodynamic limits for  $n^z$  and  $m$ . From this figure, it is clear that  $n^z$  is a universal function of  $m$  independent of the microscopic structure of the Hamiltonian. To model this universal function, we use a polynomial fit that is constrained to ensure that  $n^z \rightarrow \frac{m}{3}$  when  $m \rightarrow \frac{1}{2}$ ; the rationale for this constraint will become clear in Sec. IV. We find (Fig. 5) that the QMC results for  $n^z(m)$  are fit well by the following functional form:

$$n^z(m) = \left(\frac{1}{3} - \frac{a}{2} - \frac{b}{4}\right)m + am^2 + bm^3, \quad (11)$$

with  $a \approx 0.288$  and  $b \approx -0.306$ .

If one views this universal relationship as being a property of the low energy effective field theory of the antiferromagnetic phase, one is led to expect that the full spatial structure of the spin texture  $\Phi^z(\vec{r})$  should also be universal. More precisely, one is led to expect that this texture is dominated in a universal way by Fourier components near the antiferromagnetic wavevector. To test this, we compare the spin texture in the  $JJ'$  model and the  $JQ_3$  model, choosing the strengths of the  $J'$  interaction and the  $Q_3$  interaction so that both have the same value of  $m$ , and therefore the same value of  $n^z$ . This is shown in Fig. 6, which shows that these very different microscopic Hamiltonians have spin-textures whose Fourier transform falls on top of each other at and around the antiferromagnetic wavevector.

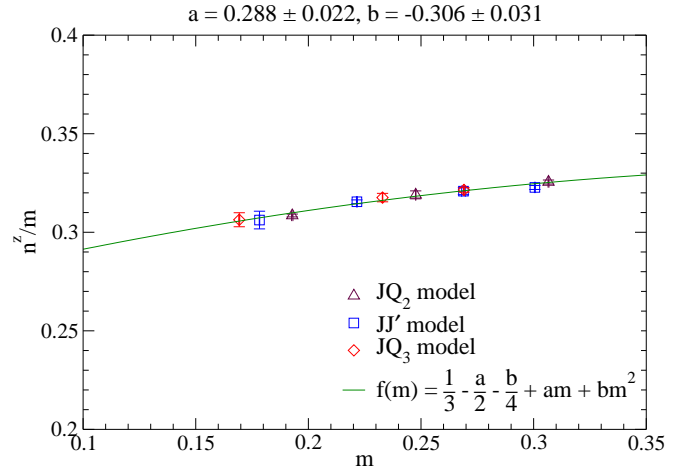


FIG. 5: Extrapolated thermodynamic values of  $n^z$  for three different models of antiferromagnets on an open lattice, plotted as function of staggered magnetisation  $m$  for the same models on periodic lattices. The former is clearly an universal function of the later. This universal function can be well approximated by a polynomial fit constrained to ensure that  $n^z(m) \rightarrow m/3$  in the limit of  $m \rightarrow \frac{1}{2}$ :  $n^z \approx (1/3 - a/2 - b/4)m + am^2 + bm^3$ , with  $a \approx 0.288$  and  $b \approx -0.306$ .

#### IV. ANALYTICAL APPROXIMATIONS

We now present three distinct analytical approaches to understanding these numerical results presented in the previous section: First, we develop a spin-wave expansion that becomes asymptotically exact for large  $S^{14}$ . Second, we explore a mean-field theory written in terms of the total spin of each sub-lattice. Finally, we describe an alternative approach in which the low-energy antiferromagnetic tower of states of a spin-1/2 antiferromagnet is described by a phenomenological rotor model<sup>17</sup> adapted to the case of a system with odd  $N_{\text{tot}}$ .

##### A. Spin-wave expansion

The leading order spin-wave calculation proceeds as usual by using an approximate representation of spin operators in terms of Holstein-Primakoff bosons. The resulting bosonic Hamiltonian is truncated to leading (quadratic) order in boson operators to obtain the first quantum corrections to the classical energy of the system.

As is standard in the spin wave theory of Néel ordered states, we start with the classical Néel ordered configuration with the Néel vector pointing along the  $\hat{z}$  axis, which corresponds to  $S_{\vec{r}}^z = \eta_{\vec{r}}S$ . We then represent the spin operators at a site  $\vec{r}$  of the square lattice in terms of canonical bosons to leading order in  $S$  as follows: For sites  $\vec{r}$  belonging to the  $A$  sublattice we write

$$S_{\vec{r}}^+ = \sqrt{2S}b_{\vec{r}}; \quad S_{\vec{r}}^z = S - b_{\vec{r}}^\dagger b_{\vec{r}}, \quad (12)$$

while on sites  $\vec{r}$  belonging to the  $B$  sublattice we write

$$S_{\vec{r}}^- = \sqrt{2S}b_{\vec{r}}^-; \quad S_{\vec{r}}^z = -S + b_{\vec{r}}^\dagger b_{\vec{r}}. \quad (13)$$

The number of bosons at each site thus represents the effect of quantum fluctuations away from the classical Néel ordered configuration.

To quadratic order in the boson operators, this expansion yields the following spin wave Hamiltonian in the general case (with arbitrary two-spin exchange couplings):

$$\begin{aligned} H_{sw} &= \epsilon_{cl} S^2 + \frac{S}{2} \mathbf{b}^\dagger \mathbf{M} \mathbf{b}, \text{ with} \\ M_{\vec{r}\vec{r}'} &= \begin{pmatrix} A_{\vec{r}\vec{r}'} & B_{\vec{r}\vec{r}'} \\ B_{\vec{r}\vec{r}'}^\dagger & A_{\vec{r}\vec{r}'} \end{pmatrix} \\ \mathbf{b}_{\vec{r}} &= \begin{pmatrix} b_{\vec{r}} \\ b_{\vec{r}}^\dagger \end{pmatrix}. \end{aligned} \quad (14)$$

Here  $\epsilon_{cl} S^2$  is the classical energy of the Néel state,  $M$  in the first line is a  $2N_{\text{tot}}$  dimensional matrix specified in terms of  $N_{\text{tot}}$  dimensional blocks  $A$  and  $B$ , and  $\mathbf{b}$  is a  $2N_{\text{tot}}$  dimensional column vector as indicated above. Elements of  $A$  and  $B$  can be written explicitly as

$$A_{\vec{r}\vec{r}'} = (Z_{\vec{r}}^U - Z_{\vec{r}'}^F) \delta_{\vec{r}\vec{r}'} + J_{\vec{r}\vec{r}'}^F, \quad (15)$$

$$B_{\vec{r}\vec{r}'} = J_{\vec{r}\vec{r}'}^U. \quad (16)$$

In the above,  $J_{\vec{r}\vec{r}'}^F$  are Heisenberg exchange couplings between two sites  $\vec{r}$  and  $\vec{r}'$  belonging to the same sub-lattice,  $J_{\vec{r}\vec{r}'}^U$  are the Heisenberg exchange couplings between sites belonging to different sublattices, and

$$Z_{\vec{r}}^U = \sum_{\vec{r}''} J_{\vec{r}\vec{r}''}^U, \quad (17)$$

$$Z_{\vec{r}}^F = \sum_{\vec{r}''} J_{\vec{r}\vec{r}''}^F. \quad (18)$$

The effects of quantum fluctuations on the classical Néel state can now be calculated by diagonalizing this Hamiltonian by a canonical Bogoliubov transformation  $\mathbb{S}$  which relates the Holstein-Primakoff bosons  $b$  to the bosonic operators  $\gamma$  corresponding to spin-wave eigenstates

$$\mathbf{b} = \mathbb{S} \Gamma, \quad \Gamma_\mu = \begin{pmatrix} \gamma_\mu \\ \gamma_\mu^\dagger \end{pmatrix}, \quad (19)$$

where  $\mathbb{S}$  is a  $2N_{\text{tot}}$  dimensional matrix that transforms from  $\mathbf{b}$  which creates and destroys bosons at specific lattice sites  $\vec{r}$  to  $\Gamma$  which creates and destroys spin-wave quanta in specific spin-wave modes  $\mu$ . Naturally, we must require that  $H_{sw}$  be *diagonal* in this new basis. We represent this diagonal form as

$$H_{sw} = \epsilon_{cl} S^2 + \frac{S}{2} \Gamma^\dagger D \Gamma, \quad (20)$$

where

$$D = \begin{pmatrix} \Lambda & 0 \\ 0 & \Lambda \end{pmatrix}, \quad (21)$$

with  $\Lambda$  denoting the diagonal matrix with the  $N_{\text{tot}}$  positive spin wave frequencies  $\lambda_\mu$  on its diagonal.

To construct a  $\mathbb{S}$  that diagonalizes  $H_{sw}$  in the  $\Gamma$  basis, we look for  $2N_{\text{tot}}$  dimensional column vectors

$$y^\mu = \begin{pmatrix} u^\mu \\ v^\mu \end{pmatrix}, \quad (22)$$

which satisfy the equation

$$M y^\mu = \epsilon_\mu \mathcal{I} y^\mu \quad (23)$$

with *positive* values of  $\epsilon_\mu$  equal to the positive spin-wave frequencies  $\lambda_\mu$  for  $\mu = 1, 2, 3 \dots N_{\text{tot}}$ . Here  $u^\mu$  and  $v^\mu$  are  $N_{\text{tot}}$  dimensional vectors,

$$\mathcal{I} = \begin{pmatrix} \mathbf{1} & \mathbf{0} \\ \mathbf{0} & -\mathbf{1} \end{pmatrix}, \quad (24)$$

and  $\mathbf{1}$  is the  $N_{\text{tot}} \times N_{\text{tot}}$  identity matrix. With these  $y^\mu$  in hand, one may obtain  $N_{\text{tot}}$  additional solutions to Eqn. 23, this time with *negative*  $\epsilon_{N_{\text{tot}}+\mu} = -\lambda_\mu$  by interchanging the roles of the  $N_{\text{tot}}$  dimensional vectors  $u_\mu$  and  $v_\mu$  in this construction. In other words, we have

$$y^{N_{\text{tot}}+\mu} = \begin{pmatrix} v^\mu \\ u^\mu \end{pmatrix}, \quad (25)$$

with  $\mu = 1, 2, 3 \dots N_{\text{tot}}$ .

We now construct  $\mathbb{S}$  by using these  $y^\mu$  (with  $\mu = 1, 2, 3 \dots 2N_{\text{tot}}$ ) as its  $2N_{\text{tot}}$  columns:

$$\mathbb{S} = (y^1, y^2, y^3 \dots y^{2N_{\text{tot}}}). \quad (26)$$

Clearly, this choice of  $\mathbb{S}$  satisfies the equation

$$M \mathbb{S} = \mathcal{I} \mathbb{S} D \quad (27)$$

Furthermore, the requirement that the Bogoliubov transformed operators  $\gamma$  obey the same canonical bosonic commutation relations as the  $b$  operators implies that  $\mathbb{S}$  must satisfy

$$\mathbb{S}^\dagger \mathcal{I} \mathbb{S} = \mathcal{I}, \quad (28)$$

This constraint is equivalent to “symplectic” orthonormalization conditions:

$$\begin{aligned} (u^\mu)^\dagger u^\nu - (v^\mu)^\dagger v^\nu &= \delta_{\mu\nu}, \\ (u^\mu)^\dagger v^\nu - (v^\mu)^\dagger u^\nu &= 0, \end{aligned} \quad (29)$$

for  $\mu, \nu = 1, 2, 3 \dots N_{\text{tot}}$ . It is now easy to see that Eqn 27 and Eqn 28 guarantee that  $H_{sw}$  is indeed diagonal in the new basis, since

$$\mathbf{b}^\dagger \mathbf{M} \mathbf{b} = \Gamma^\dagger \mathbb{S}^\dagger M \mathbb{S} \Gamma = \Gamma^\dagger \mathbb{S}^\dagger \mathcal{I} \mathbb{S} D \Gamma = \Gamma^\dagger D \Gamma. \quad (30)$$

For periodic samples, it is possible to exploit the translational invariance of the problem and work in Fourier space to obtain these spin-wave modes and their wavefunctions and calculate  $m = S - \Delta'$  correct to leading



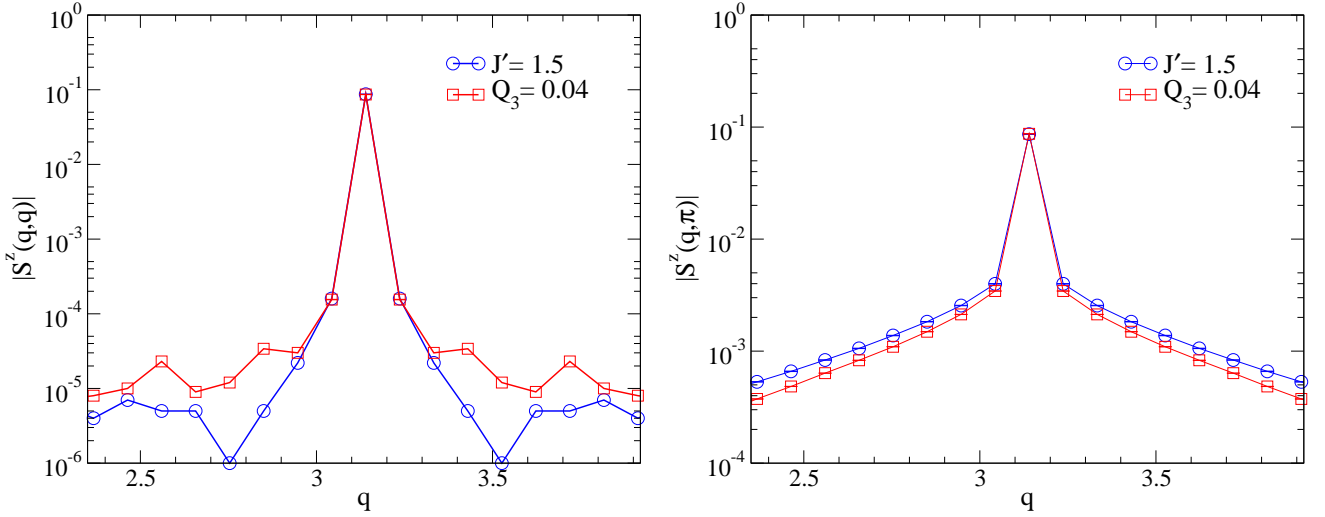


FIG. 6: Fourier transform (with antiperiodic boundary conditions assumed for convenience) of the numerically computed (for  $JJ'$  and  $JQ_3$  model with  $L = 65$ ,  $S = 1/2$ )  $\Phi^z(\vec{r})$  along cuts passing through the antiferromagnetic wavevector  $(\pi, \pi)$ . Note the universality of the results in the neighbourhood of the antiferromagnetic wavevector, which in any case accounts for most of the weight in Fourier space.

order in the spin-wave expansion—as these results are standard and well-known,<sup>15</sup> we do not provide further details here. On the other hand, the corresponding results for  $L \times L$  samples with free boundary conditions and  $N_A = N_B + 1$  do not seem to be available in the literature, and our discussion below focuses on this case.

We begin by noting that the non-zero entries in  $A$  only connect two sites belonging to the same sublattice, while those in  $B$  always connect sites belonging to opposite sublattices. As a result of this, the solutions to the equation for  $y^\mu$  can also be expressed in terms of a single function  $f_\mu(\vec{r})$  defined on sites of the lattice. To see this, we consider an auxiliary problem of finding  $\tilde{\epsilon}_\mu$  such that the operator  $A - B - \tilde{\epsilon}_\mu \eta_{\vec{r}}$  has a zero mode  $f_\mu(\vec{r})$  (as before,  $\eta_{\vec{r}}$  is  $+1$  for sites belonging to the  $A$  sublattice, and  $-1$  for sites belonging to the  $B$  sublattice).

This auxiliary problem has  $N_{\text{tot}}$  solutions corresponding to the  $N_{\text{tot}}$  roots  $\tilde{\epsilon}_\mu$  of the polynomial equation  $\det(A - B - \tilde{\epsilon}_\mu \eta_{\vec{r}}) = 0$ ; these  $\tilde{\epsilon}_\mu$  can be of either sign. To make the correspondence with the *positive*  $\epsilon_\mu$  solutions ( $u^\mu, v^\mu$ ) (with  $\mu = 1, 2, \dots, N_{\text{tot}}$ ) of the original equation  $My^\mu = \epsilon_\mu \mathcal{I}y^\mu$ , we now note that

$$\langle f_\mu | A - B | f_\mu \rangle = \tilde{\epsilon}_\mu N_\mu \quad (31)$$

where

$$N_\mu \equiv \sum_{r_A} |f_\mu(r_A)|^2 - \sum_{r_B} |f_\mu(r_B)|^2. \quad (32)$$

Since  $A - B$  is a positive (but not positive definite) operator, this implies that  $\tilde{\epsilon}_\mu$  has the same sign as  $N_\mu$  for all non-zero  $\tilde{\epsilon}_\mu$ . To make the correspondence with the positive  $\epsilon_\mu \equiv \lambda_\mu$  solutions ( $\mu = 1, 2, \dots, N_{\text{tot}}$ ) of the original

problem, we can therefore make the ansatz

$$\begin{aligned} u_{r_A}^\mu &= f_\mu(r_A) / \sqrt{N_\mu}, u_{r_B}^\mu = 0 \\ v_{r_B}^\mu &= -f_\mu(r_B) / \sqrt{N_\mu}, v_{r_A}^\mu = 0 \end{aligned} \quad (33)$$

if  $N_\mu > 0$ , or the alternative ansatz

$$\begin{aligned} u_{r_B}^\mu &= -f_\mu(r_B) / \sqrt{-N_\mu}, u_{r_A}^\mu = 0 \\ v_{r_A}^\mu &= f_\mu(r_A) / \sqrt{-N_\mu}, v_{r_B}^\mu = 0 \end{aligned} \quad (34)$$

if  $N_\mu < 0$ . Here,  $r_A$  ( $r_B$ ) denotes sites belonging to the  $A$  ( $B$ ) sublattice of the square lattice. This ansatz clearly ensures that the  $y^\mu$  (with  $\mu = 1, 2, \dots, N_{\text{tot}}$ ) obtained in this manner satisfy the original equation with positive  $\epsilon_\mu \equiv \lambda_\mu$  and are appropriately normalized.

Although this approach is not the one we use in our actual computations (see below), it provides a useful framework within which we may discuss possible zero frequency spin-wave modes, *i.e.*  $\lambda_{\mu_0} = 0$  for some  $\mu_0$ : A mode  $\mu_0$  with  $\lambda_{\mu_0} = 0$  clearly corresponds to a putative zero eigenvalue of the operator  $A - B$ . From the specific form of  $A - B$  in our problem, it is clear that such a zero eigenvalue does indeed exist, and  $f_{\mu_0}(\vec{r})$ , the corresponding eigenvector of  $A - B$ , can be written down explicitly as

$$f_{\mu_0}(\vec{r}) = 1 \quad (35)$$

Since this corresponds to the root  $\tilde{\epsilon}_{\mu_0} = 0$  of the auxiliary problem, it can *in principle* be used to obtain a *pair* of zero frequency modes  $\epsilon_{\mu_0}$  and  $\epsilon_{\mu_0 + N_{\text{tot}}}$  for the original problem of finding  $\epsilon_\mu$  and  $y^\mu$  that satisfy  $My^\mu = \epsilon_\mu \mathcal{I}y^\mu$ .

However, we need to ensure that the symplectic orthonormalization conditions (Eqn. 30) are satisfied by our construction of the corresponding  $y^{\mu_0}$  and  $y^{\mu_0 + N_{\text{tot}}}$ . This is where the restriction to a  $N_{\text{tot}} = L \times L$  lattice

with  $N_A = N_B + 1$  enters our discussion. For this case,  $N_{\mu_0} = N_A - N_B = 1$ , and we are thus in a position to write down properly normalized zero-mode wavefunctions:

$$\begin{aligned} u_{\vec{r}_A}^{\mu_0} &= f_{\mu_0}(r_A), u_{\vec{r}_B}^{\mu_0} = 0 \\ v_{\vec{r}_B}^{\mu_0} &= -f_{\mu_0}(r_B), v_{\vec{r}_A}^{\mu_0} = 0, \end{aligned} \quad (36)$$

and

$$\begin{aligned} u_r^{N_{\text{tot}}+\mu_0} &= v_r^{\mu_0}, \\ v_r^{N_{\text{tot}}+\mu_0} &= u_r^{\mu_0}. \end{aligned} \quad (37)$$

[Parenthetically, we note that the question of zero frequency spinwave modes for the more familiar case with  $N_A = N_B$  and periodic boundary conditions has been discussed earlier in the literature<sup>14</sup> and will not be considered here.]

Thus, the equation  $My^\mu = \epsilon_\mu \mathcal{I}y^\mu$  has a pair of zero modes related to each other by interchange of the  $u$  and  $v$  components of the mode, and it becomes necessary to regulate intermediate steps of the calculation with a staggered magnetic field  $\hat{z}\epsilon_h\eta_{\vec{r}}$  with infinitesimal magnitude  $\epsilon_h > 0$  in the  $\hat{z}$  direction. Denoting the corresponding  $A$  by  $A^{\epsilon_h}$ , we see that  $A^{\epsilon_h} - B$  is now a positive definite operator and does not have a zero eigenvalue. Indeed, it is easy to see from the foregoing that the corresponding eigenvalue now becomes non-zero, yielding a positive spin-wave frequency  $\lambda_{\mu_0}^{\epsilon_h} = N_{\text{tot}}\epsilon_h$ . One can also calculate the  $\mathcal{O}(\epsilon_h)$  term of  $f_{\mu_0}^{\epsilon_h}(\vec{r})$  and check that  $f_{\mu_0}^{\epsilon_h}$  tends to  $f_{\mu_0}(\vec{r})$  in a non-singular way as  $\epsilon_h \rightarrow 0$ , from which one can obtain the corresponding  $y^{\mu_0}(\epsilon_h)$  analytically in this limit. Thus, the contribution of the zero mode to all physical quantities can be obtained in the presence of a small  $\epsilon_h > 0$ , and the  $\epsilon_h \rightarrow 0$  limit of this contribution can then be taken smoothly and analytically at the end of the calculation.

In our actual calculations, we use this analytical understanding of the zero frequency spin wave mode to analytically obtain the properly regularized zero mode contribution to various physical quantities, while using a computationally convenient approach to numerically calculate the contribution of the non-zero spin wave modes. To do this, we rewrite Eqn. 23 for  $\mu = 1, 2, 3 \dots N_{\text{tot}}$  as

$$\begin{aligned} (A+B)\phi^\mu &= \lambda_\mu \psi^\mu \\ (A-B)\psi^\mu &= \lambda_\mu \phi^\mu \end{aligned} \quad (38)$$

where

$$\begin{aligned} \phi^\mu &= u^\mu + v^\mu \\ \psi^\mu &= u^\mu - v^\mu. \end{aligned} \quad (39)$$

This implies

$$(A-B)(A+B)\phi^\mu = \lambda_\mu(A-B)\psi^\mu = \lambda_\mu^2 \phi^\mu \quad (40)$$

$$(A+B)(A-B)\psi^\mu = \lambda_\mu(A+B)\phi^\mu = \lambda_\mu^2 \psi^\mu \quad (41)$$

We now decompose

$$A - B = K^\dagger K. \quad (42)$$

where

$$K = \sqrt{\omega}U. \quad (43)$$

with  $\omega$  the diagonal matrix with diagonal entries given by eigenvalues of the real symmetric matrix  $A-B$ , and  $U$  the matrix whose rows are made up of the corresponding eigenvectors.

With this decomposition, we multiply Eqn 41 by  $K$  from the left to obtain

$$K(A+B)K^\dagger \chi^\mu = \lambda_\mu^2 \chi^\mu. \quad (44)$$

with  $\chi^\mu = K\psi^\mu$ . From the solution to this equation, we may obtain the  $\phi$  as

$$\phi^\mu = (K^\dagger)\chi^\mu / \lambda_\mu. \quad (45)$$

and thence obtain  $\psi^\mu$  using Eqn 39. In order to ensure the correct normalization of the resulting  $u^\mu, v^\mu$ , we impose the normalization condition

$$(\chi^\mu)^\dagger \chi^\mu = \lambda_\mu. \quad (46)$$

Thus our computational strategy consists of obtaining eigenvalues of the symmetric operator  $K(A+B)K^\dagger$ , and using this information to calculate the  $y^\mu$  and thence the Bogoliubov transform matrix  $\mathbb{S}$ . Notwithstanding the normalization used in Eqn 46, the zero mode with  $\lambda_{\mu_0} = 0$  causes no difficulties in this approach, since we work in practice with the projection of  $K(A+B)K^\dagger$  in the space orthogonal to the zero mode. This is possible because we already have an analytic expression correct to  $\mathcal{O}(\epsilon_h)$  for  $y^{\mu_0}(\epsilon_h)$  and  $y^{N_{\text{tot}}+\mu_0}(\epsilon_h)$  corresponding to this zero mode, and do *not* need to determine these two columns of  $\mathbb{S}$  by this computational method.

We use this procedure to calculate the zero temperature boson density as

$$\langle b_{\vec{r}}^\dagger b_{\vec{r}} \rangle = \lim_{\epsilon_h \rightarrow 0} \sum_{\mu=1}^{N_{\text{tot}}} (v_{\vec{r}}^\mu(\epsilon_h))^2. \quad (47)$$

In this expression, one may use the numerical procedure outlined above to obtain the contribution of all  $\mu \neq \mu_0$  *directly* at  $\epsilon_h = 0$ , while being careful to use our analytical results for  $v^{\mu_0}(\epsilon_h)$  to obtain the limiting value of the contribution from  $\mu = \mu_0$ . This gives

$$\langle b_{\vec{r}_A}^\dagger b_{\vec{r}_A} \rangle = \sum_{\mu \neq \mu_0} (v_{\vec{r}_A}^\mu)^2 \quad (48)$$

$$\langle b_{iB}^\dagger b_{iB} \rangle = 1 + \sum_{\mu \neq \mu_0} (v_{\vec{r}_B}^\mu)^2 \quad (49)$$

Here, the distinction between sites on the  $A$  and  $B$  sublattices arises in this final result because  $\lim_{\epsilon_h \rightarrow 0} v_{\vec{r}}^{\mu_0}(\epsilon_h) = -1$  for  $\vec{r}$  belonging to the  $B$  sublattice, while  $\lim_{\epsilon_h \rightarrow 0} v_{\vec{r}}^{\mu_0}(\epsilon_h) = 0$  for  $\vec{r}$  belonging to the  $A$  sublattice.

Knowing the average boson number at each site gives us the first quantum corrections to the ground state expectation value  $\langle S^z(\vec{r}) \rangle$ :

$$\langle S^z(\vec{r}) \rangle = \eta_{\vec{r}}(S - \langle b_{\vec{r}}^\dagger b_{\vec{r}} \rangle) \quad (50)$$

This result for the spin-wave corrections to the ground state spin texture then allows us to write  $n^z = \lim_{L \rightarrow \infty} (\sum_{\vec{r}} \eta_{\vec{r}} \langle S^z(\vec{r}) \rangle) / N_{\text{tot}}$  as

$$n^z = S - \Delta \quad (51)$$

where  $\Delta$  represents the leading spin-wave correction to the classical value for  $n^z$ .

In order to obtain  $n^z$  reliably in this manner, it is important to understand the finite size scaling properties of  $\Delta$  for various values of  $J'/J$  in the striped interaction model and  $J_2/J$  in the model with next-nearest neighbour interactions. In Fig. 7, we show a typical example of this size dependence. As is clear, we find that  $\Delta$  has a non monotonic dependence on  $L$ :  $\Delta$  initially increases rapidly with size, and, after a certain crossover size  $L^*$ , it starts decreasing slowly to finally saturate to its asymptotic value. This non-monotonic behaviour is qualitatively similar to that observed in the finite size extrapolations of  $n^z$  from our QMC data earlier. To explore this unusual size dependence further and reliably extrapolate to the thermodynamic limit, we analyze the contributions to  $\Delta$  from the spin-wave spectrum in the following way: We note that there is always a monotonically and rapidly convergent  $\mathcal{O}(1)$  contribution to  $\Delta$  from the lowest frequency spin-wave mode, whose spin-wave frequency scales to zero as  $1/N_{\text{tot}}$  (for any finite  $N_{\text{tot}}$ , this is *not* an exact zero mode of the system). We dub this the ‘delta-function contribution’ and its thermodynamic limit is easy to reliably extrapolate to. In addition, there is a ‘continuum contribution’ coming from all the other spin-wave modes, each of which contributes an amount of order  $\mathcal{O}(1/N_{\text{tot}})$ . This contribution converges less rapidly to the thermodynamic limit, and also happens to be non-monotonic: it first increases quickly with increasing size, and then starts decreasing slowly to finally saturate to the thermodynamic limit.

The delta-function contribution can be fit best to a functional form

$$F_\delta(L) = b_\delta + \frac{c_\delta}{L} - \frac{a_\delta}{L^2} + \frac{d_\delta}{L^3}, \quad (52)$$

with the dominant  $1/L^2$  term accounting for the monotonic increase with  $L$ , while the continuum contribution is fit to

$$F_c(L) = b_c + \frac{c_c}{L} - \frac{a_c}{L^2} + \frac{d_c}{L^3}, \quad (53)$$

whereby the size dependence is predominantly determined by the competition between the term proportional to  $1/L$  which decreases with increasing  $L$ , and the term proportional to  $1/L^2$  which increases with increasing  $L$ .

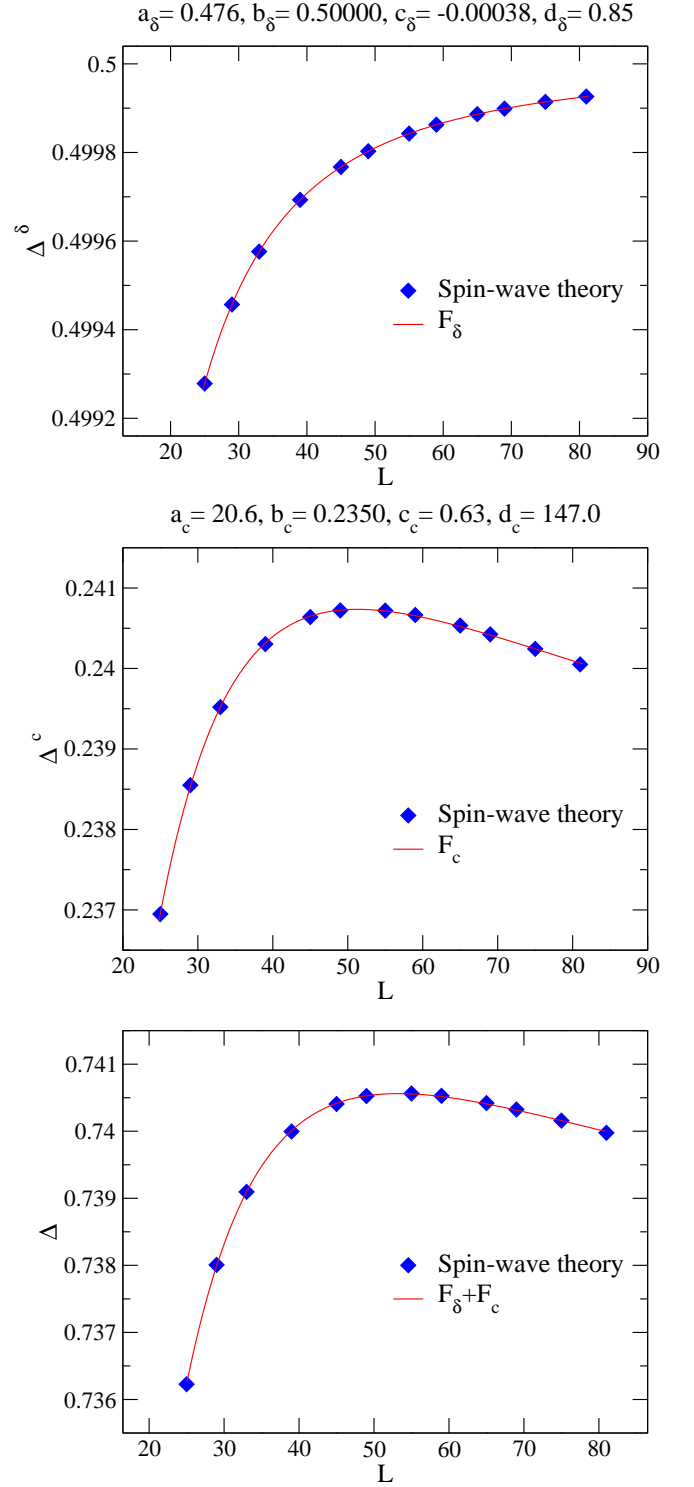


FIG. 7: A typical example of the finite size scaling of the delta-function and continuum contributions to  $\Delta$ . Note the monotonically increasing size dependence of the delta-function contribution, and the non-monotonic and more slowly converging nature of the continuum contribution. Due to this difference in their behaviour, we find it more accurate to separately fit each of these contributions to a polynomial in  $1/L$  and use this to obtain the thermodynamic limit of the total  $\Delta$ . Here  $F_{\delta/c}(L) = b_{\delta/c} + c_{\delta/c}/L - a_{\delta/c}/L^2 + d_{\delta/c}/L^3$ .



This gives rise to non-monotonic behaviour whereby the continuum contribution first increases rapidly and then decreases slowly beyond a crossover length  $L^*$  to finally saturate to its infinite volume limit. We also find that the length  $L^*$  gets larger as we deform away from the pure square lattice antiferromagnet, making it harder to obtain reliable extrapolations to the thermodynamic limit.

Using such careful finite-size extrapolations to obtain  $\Delta$  for various values of  $J_2/J$  and  $J'/J$ , we compare the result with  $\Delta'$  calculated analytically. Specifically, we now ask if the universality seen in our QMC results is reflected in these semiclassical spin-wave corrections to  $n^z$  and  $m$ . The answer is provided by Fig. 8, which shows that the numerically obtained spin-wave corrections apparently satisfy a universal linear relationship

$$\Delta - \Delta' \approx 1.003 + 0.013\Delta' \quad (54)$$

as one deforms away from the pure square lattice antiferromagnet in various ways.

What does this imply for  $n^z(m)$  to leading order in  $1/S$ ? To answer this, we note that

$$\frac{n^z}{m} = 1 - \frac{\Delta - \Delta'}{S} + \mathcal{O}(S^{-2}) \quad (55)$$

Using our numerically established universal result to relate  $\Delta - \Delta'$  to  $\Delta'$  and thence to  $m$  itself, we obtain the universal relationship

$$n^z = \alpha m + \beta m^2 \quad (56)$$

with  $\alpha \approx 0.987 - 1.003/S$  and  $\beta \approx 0.013/S$ . However, being a large- $S$  expansion, spin-wave theory is unable to give a quantitatively correct prediction for  $n^z(m)$  for the  $S = 1/2$  case.

Finally, we use our spin-wave predictions for the ground-state spin texture to look at the Fourier transform of the spin-texture for various deformations of the pure antiferromagnet. The results are shown in Fig. 9, which demonstrates that spin-wave theory also predicts that the Fourier transform of the spin-texture near the antiferromagnetic wave-vector is a universal function of the wavevector; this provides some rationalization for the observed universality of the Fourier transformed spin texture seen in our QMC numerics.

## B. Sublattice-spin mean-field theory

We now turn to a simple mean-field picture in terms of the dynamics of the total spins  $\vec{S}_A$  and  $\vec{S}_B$  of the  $A$  and  $B$  sublattices respectively. When  $N_A = N_B + 1$ , it is clearly appropriate to assume that the total spin

quantum number of  $\vec{S}_A$  is  $S_B + 1/2$  while the total spin quantum number of  $\vec{S}_B$  should be taken to be  $S_B$ , where  $S_B = N_B/2$  tends to infinity in the thermodynamic limit.

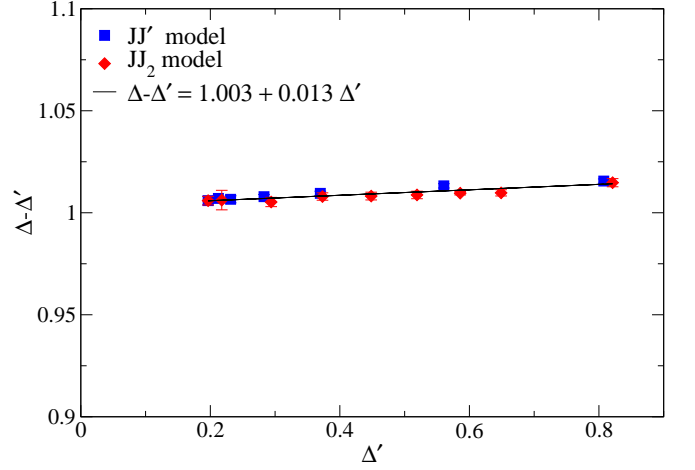


FIG. 8:  $\Delta - \Delta'$ , the difference between the leading spin wave corrections to  $n^z$  and  $m$ , plotted against the leading spin-wave corrections  $\Delta'$  to  $m$  for the  $JJ'$  and  $JJ_2$  models described in the text.

Hamiltonian that describes the low energy part of the spectrum:

$$H_{MF} = J_{MF} \vec{S}_A \cdot \vec{S}_B \quad (57)$$

with  $J_{MF} > 0$ . Within this mean-field treatment, the  $S_{\text{tot}} = 1/2$ ,  $S_{\text{tot}}^z = 1/2$  ground state that we focus on in our numerics is thus the  $S_{\text{tot}} = 1/2$ ,  $S^z = 1/2$  state obtained by the quantum mechanical addition of angular momenta  $S_B$  and  $S_B + 1/2$ . Within this mean-field theory,  $n^z$  is modeled as the expectation value of  $(S_A^z - S_B^z)/N_{\text{tot}}$  in this state, which can be readily obtained in closed form using the following standard result for the minimum angular momentum state  $|J = j_1 - j_2, m_J\rangle$  state obtained by the addition of angular momenta  $j_1$  and  $j_2$  (with  $j_1 \geq j_2$ ):

$$\langle j_1, m_1; j_2, m_2 | J, m_J \rangle = \rho_J c_{m_1, m_2}^{J, m_J} \quad (58)$$

with

$$\rho_J = \sqrt{\frac{(2J+1)!(2j_2)!}{(2j_1+1)!}} \quad (59)$$

and

$$c_{m_1, m_2}^{J, m_J} = (-1)^{j_2+m_2} [(j_1+m_1)!((j_1-m_1)!)]^{1/2} [(j_2+m_2)!(j_2-m_2)!(J+m_J)!(J-m_J)!]^{-1/2} \quad (60)$$

for  $m_1 + m_2 = m_J$  and  $c_{m_1, m_2}^{J, m_J} = 0$  otherwise.

In our case,  $j_1 = S_B + 1/2$ ,  $j_2 = S_B$ ,  $J = 1/2$ ,  $m_J = 1/2$ , and  $n^z = \langle m_1 - m_2 \rangle_{J, m_J} / N_{\text{tot}}$  can therefore be readily calculated to obtain

$$n^z = \left( \frac{2}{3} S_B + \frac{1}{2} \right) / N_{\text{tot}} \quad (61)$$

within this phenomenological approach.

On the other hand, when  $N_A = N_B$ , we may also calculate  $m^2 = \langle (\vec{S}_A - \vec{S}_B)^2 \rangle_{J=0} / N_{\text{tot}}^2$  within the same sublattice-spin approach

$$m^2 = (4S_B^2 + 4S_B) / N_{\text{tot}}^2. \quad (62)$$

This allows us to compute the ratio  $n^z/m$  in the thermodynamic limit:

$$n^z = \frac{1}{3}m + \mathcal{O}\left(\frac{1}{N_{\text{tot}}}\right) \quad (63)$$

Is there a limit in which this sublattice-spin mean-field theory is expected to give exact results? To answer this, we note that the sublattice-spin model represents the Hamiltonian of an infinite-range model in which *every*  $A$  sublattice-spin interacts with *every*  $B$  sublattice-spin via a *constant* (independent of distance) antiferromagnetic exchange coupling  $J_{MF}$ . Thus, our mean-field theory is expected to become asymptotically exact in the limit of infinitely long-range unfrustrated couplings. In this limit, we also expect  $m \rightarrow 1/2$ , and thus, our mean field theory predicts that  $n^z \rightarrow m/3$  when  $m \rightarrow 1/2$ . This is the constraint that we built into our choice of polynomial fit for  $n^z(m)$  in Sec. III.

### C. Quantum rotor Hamiltonian

When any continuous symmetry is broken, the corresponding order parameter variable becomes very “heavy” in a well-defined sense.<sup>14</sup> The long-time, slow dynamics of this heavy nearly classical variable is controlled by an effective “mass” that diverges in the thermodynamic limit.

For a Néel ordered magnet, the order parameter is the Néel vector  $\vec{n}$ . In the usual case of an antiferromagnet with an even number of  $S = 1/2$  moments, the low-energy effective Hamiltonian that controls the orientational dynamics of the Néel vector  $\vec{n}$  is

$$H_{\text{rotor}} = \frac{\vec{L} \cdot \vec{L}}{2\chi N_{\text{tot}}} \quad (64)$$

where  $\vec{L}$  is the angular momentum conjugate to the “quantum rotor” coordinate  $\hat{n} \equiv \vec{n}/|\vec{n}|$ ,  $\chi$  is the uniform susceptibility per spin, and  $N_{\text{tot}}$  is the total number of spins.

What about our case with  $N_A = N_B + 1$  and an odd number of spins  $N_{\text{tot}}$ ? Following earlier work on quantum

rotor descriptions of insulating antiferromagnets doped with a single mobile charge-carrier<sup>17</sup>, we postulate that the correct rotor description of our problem is in terms of a rotor Hamiltonian in which  $\vec{L}$  is replaced by the angular momentum operator  $\vec{L}'$  conjugate to a quantum rotor coordinate  $\hat{n}$  that now parametrizes a unit-sphere with a fundamental magnetic monopole at its origin.<sup>18</sup> In other words, we postulate a low-energy effective Hamiltonian

$$H_{\text{rotor}}^{1/2} = \frac{\vec{L}' \cdot \vec{L}'}{2\chi N_{\text{tot}}} \quad (65)$$

where the superscript reminds us that the lowest allowed angular momentum quantum number  $l$  of the modified angular momentum operator  $\vec{L}'$  is  $l = 1/2$ .

In the notation of Ref 18, the angular wavefunction of the  $l = 1/2$ ,  $m_l = 1/2$  ground state of this modified rotor Hamiltonian is the *monopole harmonic*  $Y_{1/2, 1/2, 1/2}(\theta, \phi)$ . To model  $\langle n^z \rangle_{\uparrow}$ , we must compute the expectation value  $\langle \cos(\theta) \rangle_{1/2, 1/2, 1/2}$  and multiply this result by  $m \equiv |\vec{n}|$ . To do this we note that

$$|Y_{1/2, 1/2, \pm 1/2}(\theta, \phi)|^2 = \frac{1}{4\pi} (1 \pm \cos(\theta)), \quad (66)$$

which immediately implies

$$\langle n^z \rangle_{\uparrow} = m \int d\cos(\theta) d\phi \cos(\theta) |Y_{1/2, 1/2, 1/2}(\theta, \phi)|^2 = \frac{1}{3}m \quad (67)$$

Thus, a more general phenomenological approach that goes beyond sublattice-spin mean-field theory but ignores all non-zero wavevector modes also gives

$$n^z = \frac{m}{3}. \quad (68)$$

Since our QMC data show clear deviations from this result, we conclude that such non-zero wavevector modes are essential for a correct calculation of the universal function  $n^z(m)$ .

## V. DISCUSSION

A natural question that arises from our results is whether the universal ground state spin texture we have found here can be successfully described using an effective field theory approach of the type used recently by Eggert and collaborators for studying universal aspects of the alternating order induced by missing spins in two dimensional  $S = 1/2$  antiferromagnets.<sup>19</sup> This approach uses a non-linear sigma-model description of the local antiferromagnetic order parameter, with lattice scale physics only entering via the values of the stiffness constant  $\rho_s$  and the transverse susceptibility  $\chi_{\perp}$ , and the presence of the vacancy captured by a local term in the action. An analogous treatment for our situation would need two things—one is a way of restricting attention to averages

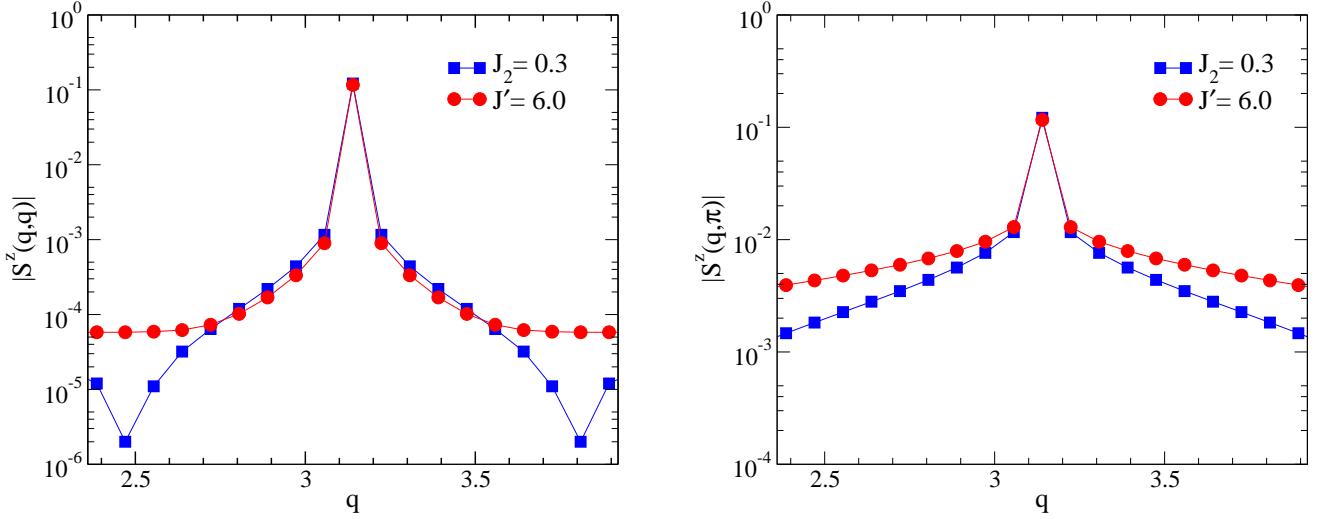


FIG. 9: Fourier transform (with antiperiodic boundary conditions assumed for convenience) of the spin-wave result for  $\Phi^z(\vec{r})$  (assuming  $S = 3/2$  and calculated using  $L = 75$  for  $JJ_2$  and  $JJ'$  model) along cuts passing through the antiferromagnetic wavevector  $(\pi, \pi)$ . Note the nearly universal nature of the results in the neighbourhood of the antiferromagnetic wavevector, which in any case accounts for most of the weight of the transformed signal.

in the  $S_{\text{tot}} = 1/2$  component  $|G\rangle_{\uparrow}$  of the ground state doublet, and the other is an understanding of the right boundary conditions or boundary terms in the action, so as to correctly reflect that fact that our finite sample has open boundaries. We leave this as an interesting direction for future work, which may shed some light on the role of non-zero wavevector modes that were left out of the rotor description of the earlier section.

## VI. ACKNOWLEDGEMENTS

We thank L. Balents, A. Chernyshev, M. Metlitski, S. Sachdev, R. Shankar and R. Loganayagam

for useful discussions. The work of KD was supported by Grants DST-SR/S2/RJN-25/2006 and IFC-PAR/CEFIPRA Project 4504-1, and that of AWS by NSF Grant No. DMR-1104708. The numerical calculations were carried out using computational resources of TIFR. AWS gratefully acknowledges travel support from the Indian Lattice Gauge Theory Initiative at TIFR.

- 
- <sup>1</sup> H. Neuberger and T. Ziman, Phys. Rev. B **39**, 2608(1989).
  - <sup>2</sup> S. R. White and A. L. Chernyshev, Phys. Rev. Lett. **99**, 127004 (2007).
  - <sup>3</sup> A. W. Sandvik, Phys. Rev. B **56**, 11678 (1997).
  - <sup>4</sup> B. B. Beard, R. J. Birgeneau, M. Greven, and U.-J. Wiese, Phys. Rev. Lett. **80**, 1742 (1998).
  - <sup>5</sup> E. Lieb and D. C. Mattis, J. Math. Phys. **3**, 749 (1962).
  - <sup>6</sup> K. Hoglund Ph.D thesis (2010); K. Hoglund and A. W. Sandvik, unpublished.
  - <sup>7</sup> S. Wenzel and W. Janke, Phys. Rev. B **79**, 014410(2009).
  - <sup>8</sup> A. W. Sandvik, Phys. Rev. Lett. **98**, 227202 (2007).
  - <sup>9</sup> J. Lou, A. W. Sandvik, and N. Kawashima, Phys. Rev. B **80**, 180414 (2009).
  - <sup>10</sup> A. Banerjee and K. Damle, J. Stat. Mech. (2010) P08017.
  - <sup>11</sup> A. W. Sandvik, Phys. Rev. Lett. **95**, 207203 (2005).
  - <sup>12</sup> A. W. Sandvik, and H. G. Evertz, Phys. Rev. B **82**, 024407 (2010).
  - <sup>13</sup> A. W. Sandvik, Phys. Rev. Lett. **83**, 3069 (1999).
  - <sup>14</sup> P. W. Anderson, Phys. Rev. **86**, 694 (1952).
  - <sup>15</sup> P. Chandra and B. Doucot, Phys. Rev. B **38**, 9335, 1988
  - <sup>16</sup> J. H. P. Colpa, Physica A **2**, 134, 377-416 (1986); J. H. P. Colpa, Physica A **2**, 134, 417-422 (1986)
  - <sup>17</sup> S. Chandrasekharan, F.-J. Jiang, M. Pepe, and U.-J. Wiese, Phys. Rev. D **78**, 077901 (2008).
  - <sup>18</sup> T. T. Wu and C. N. Yang, Nuc. Phys. **B107**, 365 (1976); Phys. Rev. D **16**, 1018 (1977).
  - <sup>19</sup> S. Eggert, O.F. Syljuåsen, F. Anfuso, M. Andres, Phys. Rev. Lett. **99**, 097204 (2007).